

# Oil & Natural Gas Technology

DOE Award No.: DE-FE 0009963

## Quarterly Research Performance Progress Report (Period ending 9/31/2013)

**Measurement and Interpretation of Seismic Velocities and Attenuations  
in Hydrate-Bearing Sediments**

**Project Period (10/1/2012 to 9/30/2015)**

Submitted by:

PI: Michael Batzle

Colorado School of Mines

DUNS #010628170.

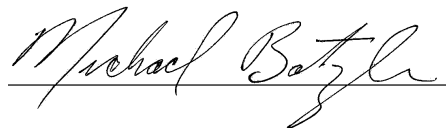
1500 Illinois Street

Golden, CO 80401

e-mail: [mbatzle@mines.edu](mailto:mbatzle@mines.edu)

Phone number: (303) 384-2067

Submission Date: 7/31/2013



Prepared for:

United States Department of Energy  
National Energy Technology Laboratory



**Office of Fossil Energy**

***Disclaimer:***

This report was prepared as an account of work sponsored by an agency of the United States Government. Neither the United States Government nor any agency thereof, nor any of their employees, makes any warranty, express or implied, or assumes any legal liability or responsibility for the accuracy, completeness, or usefulness of any information, apparatus, product, or process disclosed, or represents that its use would not infringe privately owned rights. Reference herein to any specific commercial product, process, or service by trade name, trademark, manufacturer, or otherwise does not necessarily constitute or imply its endorsement, recommendation, or favoring by the United States Government or any agency thereof. The views and opinions of authors expressed herein do not necessarily state or reflect those of the United States Government or any agency thereof.

***Abstract:***

Measurement and Interpretation of Seismic Velocities and Attenuations  
in Hydrate-Bearing Sediments

Grant/Cooperative Agreement DE-FE 0009963.

During this project period, we have concentrated on the measurements needed to characterize hydrate growth and location. The exact morphology of hydrates within pore spaces and between grains is critical in determining physical properties. Hence we have concentrated on characterizing distributions of phases as well as property measurements.

- CT imaging processing was improved to distinguish liquid and hydrate phases
- THF hydrates grown from solution occupy the central portions of the pore space
- Ultrasonic measurements confirm the 'loadbearing' models of THF hydrates
- BaCl<sub>2</sub> brines cling to mineral surfaces influencing hydrate nucleation
- NMR measurements on bulk samples demonstrate the distinctions among liquids, hydrates, and mixtures.

Growth of THF hydrate is now routine in our laboratory. Our characterization techniques continue to improve and we are extending our methods towards production of methane hydrates.

**Contents:**

Disclaimer ..... 2

Abstract ..... 3

Contents ..... 4

Figures ..... 5

Tables ..... 5

Executive Summary ..... 6

Accomplishments ..... 7

    Background / pore scale models ..... 8

    Stage 1: THF hydrates ..... 12

    Experimental Methodology ..... 10

    Micro X-ray Computed Tomography (CT) ..... 10

    Ultrasonic Measurements ..... 11

    MXCT Imaging ..... 13

    Ultrasonic Results ..... 15

    Nuclear Magnetic Resonance (NMR) ..... 18

Plans ..... 20

Participants and Collaborating Organizations..... 21

Changes / Problems ..... 22

Special Reporting Requirements ..... 22

Budgetary Information ..... 22

References ..... 23

Milestone Status ..... 25

**Figures:**

|  |    |
|--|----|
| Figure 1. Effective media models for the effect of hydrate formation .....           | 9  |
| Figure 2. Micro CT scanner with hydrate assembly .....                               | 10 |
| Figure 3. Sample for ultrasonic velocity measurements .....                          | 11 |
| Figure 4. Experimental setup for ultrasonic velocity measurements .....              | 12 |
| Figure 5. CT images of glass bead sample with initial hydrate saturation of 80% .... | 13 |
| Figure 6. Image processing workflow for MXCT images .....                            | 15 |
| Figure 7. Histograms, gray values & differential CT images .....                     | 16 |
| Figure 8. Velocities of P-, S1- and S2-wave for a sample with $S_h=40\%$ .....       | 16 |
| Figure 9. Effective medium model with P-wave velocities.....                         | 17 |
| Figure 10. Raw NMR data for pure THF and hydrate mixtures .....                      | 19 |
| Figure 11. Derived T2 relaxation times for the THF mixtures and hydrates. ....       | 20 |

**Tables:**

|  |    |
|--|----|
| Table 1. Density of sample components .....                  | 14 |
| Table 2. Ultrasonic velocities after hydrate formation ..... | 17 |

## **Executive Summary:**

Tetrahydrofuran (THF) hydrate can now be grown routinely in our lab. This hydrate is only a proxy for the naturally occurring methane hydrate, but is simpler to handle and apply in the laboratory. In alignment with our project plans, we are completing THF hydrate measurements as we extend our capabilities to grow CH<sub>4</sub> hydrate.

We continue to extend Micro X-ray Computed Tomography (micro CT) analysis process to give us better resolution between phases of low density contrast. The CT analysis demonstrated that THF hydrate when formed out of solution is formed in the pore space away from the grain surfaces. It can be distributed according to either the pore filling or load-bearing model of the effective medium theory. To distinguish between these two models, ultrasonic velocities were measured and compared to rock physics models.

The measured ultrasonic velocities coincide with the effective medium models by Ecker et al., 1998 and Helgerud et al., 1999. P and S-wave velocities are close to the load bearing and the envelope-cementing model. Since the MXCT images clearly showed that the THF hydrate is distributed in the pore space away from the grain surfaces this data is interpreted as according to the load-bearing model.

T scans also indicate that the barium chloride –rich brine continues to coat the mineral grains as hydrates are grown in the bulk pore space. When hydrates grow, the BaCl<sub>2</sub> is excluded and the concentration in any remaining water increases. As shown in previous reports, the BaCl<sub>2</sub> content can depress freezing point and slightly modify the stability field of the hydrate-brine system. Ultrasonic velocity measurements have confirmed the temperature shift in hydrate formation.

It has become apparent that the exact physical state of our hydrate composite will be critical in controlling the physical properties. For example, incomplete conversion to hydrate can leave pockets of liquid water (brine) or THF in the pore space. Nuclear Magnetic Resonance (NMR) is one tool that can be used to quantify the proportions of liquids and hydrates within the sample. A sequence of NMR tests are now being performed. Calibration measurements on bulk water, liquid THF, and THF hydrate composites are underway that will allow us to quantify phase contents. Mineral surface conditions (clean versus coated) will also influence hydrate growth and location, and NMR measurements will assist by monitoring water mobility during hydrate growth.

## ***Accomplishments***

Laboratory measurements were conducted to obtain information about the distribution of hydrate in the pore space of synthetic coarse-grained sediments. Tetrahydrofuran (THF) was used as a guest molecule as THF hydrate is a proxy for methane hydrate, a very common hydrate in nature. We performed micro X-ray computed tomography (MXCT) and ultrasonic velocity measurements on laboratory formed glass-bead samples. Both measurements, MXCT images and ultrasonic velocity measurements, confirmed that hydrate formed out of solution within the pore space away from the grain surfaces. The data was compared to effective medium models and appears to be in accordance with the model “load bearing” after Ecker et al. (1998). Based on this knowledge, it may be possible to calibrate seismic measurements and well logging data, e.g. for calculating the amount of gas stored in a hydrate reservoir. This information is important to decide about the producibility of a hydrate reservoir and to develop economic and safe production schemes.

## ***Introduction***

Gas hydrates occur naturally in shallow sediments in Arctic permafrost regions and beneath the seafloor at continental slopes. These environments meet the hydrates’ required stability conditions of low temperature and high pressure. The estimated amount of natural gas, mainly methane, stored in hydrate reservoirs exceeds the amount of natural gas stored in conventional resources by at least one order of magnitude (Meyer, 1981, Dobrynin et al., 1981, Collett et al., 2009). The vast quantity of methane contained in gas hydrates and their widespread geographic occurrence attracts attention from scientists, governmental institutions and major energy companies. Anderson et al. (2008) and Dallimore et al. (2008) proved that gas hydrate can be developed with existent oil and gas technology. Physical properties of gas-hydrate bearing sediments need to be known to identify and economically produce methane from hydrate reservoirs.

The most common ways to characterize and quantify gas hydrates in nature are seismic surveys and well logging. In order to calibrate and interpret these field measurements, laboratory studies are necessary to gain knowledge about bulk physical properties of hydrate-bearing sediments. At the moment, scientists are able to predict the existence of hydrates from geophysical measurements, however, they can not yet give a reliable estimate of hydrate saturation based on either seismic data or well logs (Collett et al., 2009). Thus, the amount of hydrate stored in a reservoir remains unknown. Information about the distribution of gas hydrate in the rock is necessary to determine hydrate saturation.

Gas hydrates occur as massive zones and lenses in fractures and fine grained material as well as distributed in the pore space of coarse grained porous media. Different distributions of gas hydrate in the pore space affect the rock physics properties. Thus, it is necessary to investigate hydrate-sediment interaction as well as pure hydrates (Yun,

2005). Hydrate distribution in the pore space depends mainly on the formation method. Two methods are found in nature: formation from methane dissolved in water and formation from methane in the gaseous phase (Collett et al., 2009). These two possible formation methods are believed to result in different pore-scale distribution of hydrate (Ecker et al., 1998). Hydrate formed from methane gas tends to form at the grain surfaces and grain contacts while hydrate formed out of solution seems to form in the pore space with little or no contact to the sediment grains.

In this period, we continued to concentrate on the pore-scale distribution of gas hydrates in synthetic coarse-grained porous media. Coarse grained sand reservoirs, as they exist in permafrost regions, are relatively easy to access and thus most likely to permit methane production from gas hydrates (Boswell and Collett, 2006).

The project goal is to determine the pore-scale distribution of hydrate formed out of solution. Micro X-ray computed tomography (MXCT) images were utilized for that purpose. In addition, we investigate the influence of hydrate saturation and distribution on ultrasonic velocities. The relation between pore-scale distribution, formation method and ultrasonic velocities is essential to determine the amount of hydrate in a reservoir from geophysical field data

## ***Background***

### *Pore Scale Distribution Models*

Theoretical models correlate different pore-scale hydrate distributions and their impact on ultrasonic velocities. One such model is the effective medium theory which was applied to hydrate-bearing sediments by Ecker et al. (1998) and Helgerud et al. (1999).

For reference, Figure 1 shows the four different pore-scale distributions according to the effective medium model for hydrates in sediment: contact cementing, envelope cementing, pore filling and load bearing. The envelope cementing model shows a drastic increase in ultrasonic velocities even for small amounts of hydrate in the pore space whereas hydrate formed according to the pore filling model shows a much smaller influence on the ultrasonic velocities. Hydrate formation from free gas appear to create grain-cementing hydrate (Ecker et al., 1998). Hydrate formed from gas dissolved in water seems to have little or no contact with the sediment grains (Rydzny and Batzle, 2011).



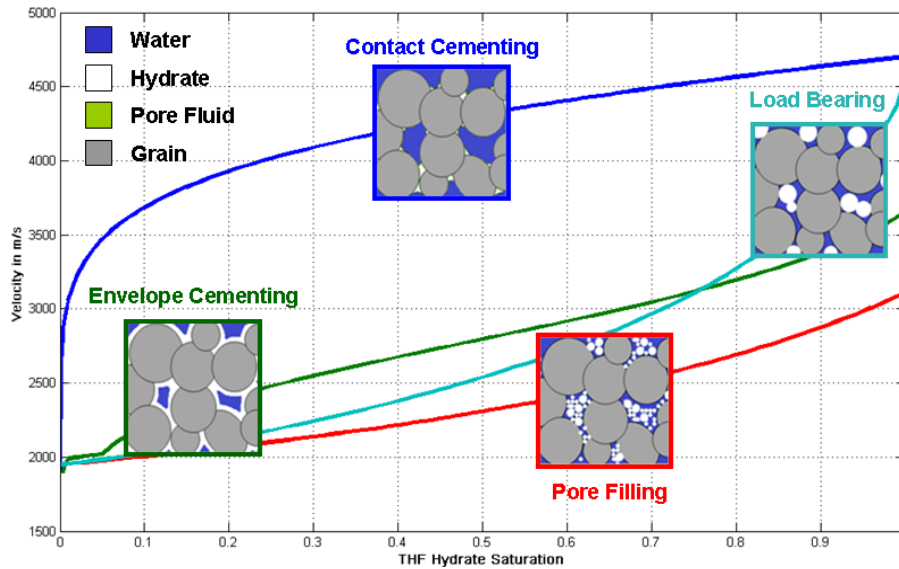


**Figure 1: Effective medium theory after Ecker et al. 1998, modified by Helgerud et al., 1999: different distributions of hydrate in the pore space and their influence on ultrasonic velocities, conceptual figures from Rydzy and Batzle, 2011**

The experimental setup inside the MXCT scanner is still being tested for accurate control of pressure and temperature, thus scanning methane hydrate samples is not possible. Methane hydrate either needs to be cooled to  $-78.7^{\circ}\text{C}$  to be stable under atmospheric pressure (Sloan and Koh, 2008) or requires a pressure of 4 MPa to be stable at  $4^{\circ}\text{C}$  (Carroll, 2009). Therefore, we use Tetrahydrofuran (THF) which forms hydrates at atmospheric pressure and temperatures of  $4^{\circ}\text{C}$  (Sloan and Koh, 2008).

### ***Stage 1: THF hydrate***

THF is a heterocyclic ether with the molecular formula  $\text{C}_4\text{H}_8\text{O}$ . THF is completely miscible in water (Sloan and Koh, 2008) and thus widely used to resemble methane hydrate formation out of solution (e.g. Pearson et al., 1986, Collett et al., 2000, Yun et al., 2005). The controlled synthesis of methane hydrate from the aqueous phase is ambitious, mainly because of the low solubility of methane in water ( $1.5 \cdot 10^{-3}$  mol methane per 1 mol water at 5 MPa and  $25^{\circ}\text{C}$ , Lide and Frederikse, 1995). This low solubility necessitates long experimental time for hydrate formation from the aqueous phase (Spangenberg et al., 2005). Lee et al. (2007) demonstrated that THF and methane hydrates exhibit similar macroscale mechanical, electrical and thermal characteristics. THF has the advantage of providing close control on the hydrate saturation by varying the stoichiometric THF- $\text{H}_2\text{O}$  mixture without having the long formation history of methane hydrate.

## ***Experimental Methodology***

### *Micro X-Ray Computed Tomography*

The MicroXCT-400 apparatus from XRadia continues to be used for the MXCT measurement. The initial sample holder consisting of two dry-ice containers at the top and bottom and a plastic tube for the sample in between has been used to perform the measurements (Figure 2). This setup provided a temporary cooling of the sample to keep the hydrate stable long enough to scan it. Data acquisition for one tomography took about 20 minutes, allowing the examination of hydrate dissociation.

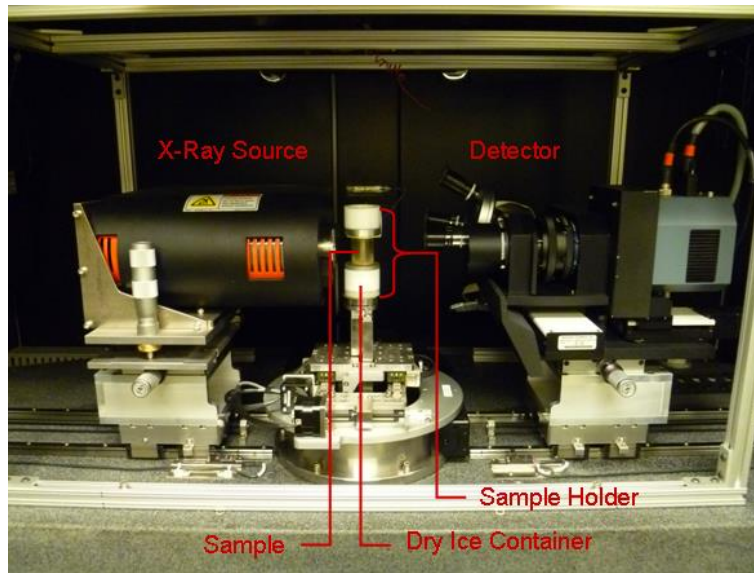


**Figure 2: Experimental setup inside the CT scanner**

The hydrate was formed outside of the CT scanner prior to the image acquisition. The samples were formed in cylindrical plastic containers with a volume of 1.1 ml. The laboratory samples characterized by MXCT measurements consisted of borosilicate glass beads (diameter: 1 mm), de-ionized water, THF and barium chloride. All samples had a porosity around 30%. H<sub>2</sub>O-THF ratios resulting in 20%, 40%, 60%, 80% and 100% hydrate saturation have been used. After combining all sample compounds, the sample was sealed to prevent the THF from volatilizing and water from evaporating. The samples were then stored in a freezer, where they were slowly cooled to -25°C over a time period of about 48 hours. The samples were cooled to -80°C for one hour to avoid immediate dissociation of the hydrate before scanning.

MXCT measurements allow the distinction between materials with different bulk densities. They provide insight into the distribution of different sample components in the pore space. In contrast to sediment grains, glass beads have uniform density (2.23 g/cm<sup>3</sup>), X-ray absorbance value, and shape. These properties make it easier to interpret the bulk MXCT images. To enhance the density contrast between ice and hydrate, 5 wt% barium

chloride was added to the fluid mixture. The density contrast for a sample with 60% hydrate saturation for example is increased by five times when barium chloride is added. As the hydrates form, barium chloride is excluded from the hydrate structure and freezes within the water phase.

The dissociation process was monitored by taking six consecutive tomographies. For each tomography, 200 images were taken with an angular increment of  $1^\circ$ . The low number of images and the big angular increment were chosen in order to minimize the scanning time. An X-ray source voltage of 90 keV and a power of 7 Watt were used for the tomographies. The scanning time for one series of six tomographies was about 2 hours.

The output data of the MXCT scanner are gray scale images. Different gray values represent materials with different bulk densities. Dark gray areas indicate low bulk density, light gray to white areas correspond to high bulk density.

### *Ultrasonic Velocity Measurements*

The basic principle of ultrasonic velocity measurements is to send an acoustic signal through the sample and measure the signals travel time through the sample. The setup of a sample with an ultrasonic transducer at each end is illustrated in Figure 3.

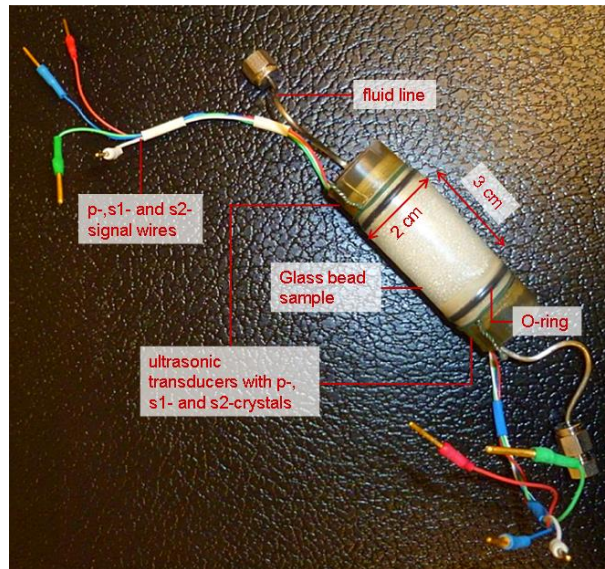


**Figure 3: Sample for ultrasonic velocity measurements**

The transducer contains piezoelectric lead zirconate titanate (PZT) crystals for each wave: P, S1 and S2. S1 and S2 are S-waves polarized orthogonal to each other. The signal is excited by a pulser which sends an electric impulse to the ultrasonic transducer. The electric impulse generates a mechanical strain. The mechanical strain is an ultrasonic signal with a frequency of about 1 MHz that propagates through the sample and is

recorded by a transducer at the other end of the sample and then visualized on a digital phosphor oscilloscope. The samples have a total volume of 9.4 ml and are composed similarly to the ones used for MXCT measurements.

The ultrasonic experiments were performed in a pressure vessel (Figure 4). Two thermocouples recorded the temperature inside the pressure vessel but outside of the sample at its top and bottom. The pressure vessel was encased by a cooling coil connected to a cooling bath for regulating the temperature of the sample. THF-water-barium-chloride mixture was pumped in the sample at a pore pressure of 100 psi. The confining pressure was increased to 535 psi. The resulting differential pressure was 435 psi (3 MPa). Measurements were conducted on samples with THF-hydrate saturations of 40%, 60%, 80% and 100%.

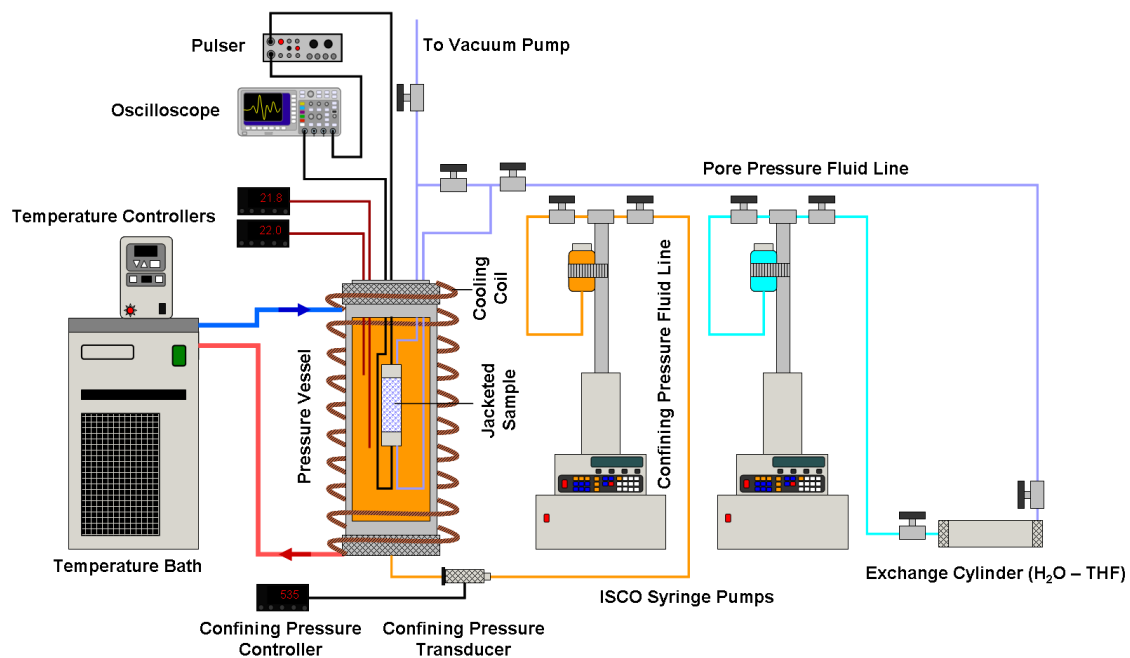


**Figure 4: Experimental setup for ultrasonic velocity measurements, modified from Rydzy and Batzle, 2011**

After the hydrate-forming mixture was pumped in the sample, the temperature was gradually decreased below hydrate stability temperature. The cooling process was faster in the beginning (4.5°C per hour) but the cooling rate was decreased to 0.7°C per hour when the hydrate equilibrium temperature was reached. Waveforms for all three wave types (P, S1, S2) were recorded during the cooling process for each 1°C interval. At temperatures close to the hydrate stability zone, waveforms were recorded more frequently. The cooling process was continued until hydrate formed in the sample which was indicated by a significant increase in all three velocities. When the hydrate formation started, the temperature was kept constant until the velocities stabilized. After the cooling process and hydrate formation, the sample was warmed slowly to room temperature at a

rate of 4.3°C per hour. Thereby ultrasonic waveforms were recorded to monitor the dissociation process.

First arrival times were picked from the waveforms recorded by the oscilloscope. The sample length was determined from MXCT images. Ultrasonic velocities can be determined from arrival time and sample length:

$$v = \frac{l}{t - t_0} \quad (1)$$

Where  $l$  is the length of the sample,  $t$  is the first arrival time and  $t_0$  is the dead time. The length of each sample was measured with the micro X-ray CT scanner.

### *MXCT Imaging*

The reconstructed images (Figure 5) contain information but for obtaining a better image quality and quantitative information from the CT images, further steps are required. Because of its low density (Table 1), THF hydrate and ice appear as low gray-value areas in the CT image whereas water with barium chloride and precipitated barium chloride show higher gray values caused by their higher density (Table 1).

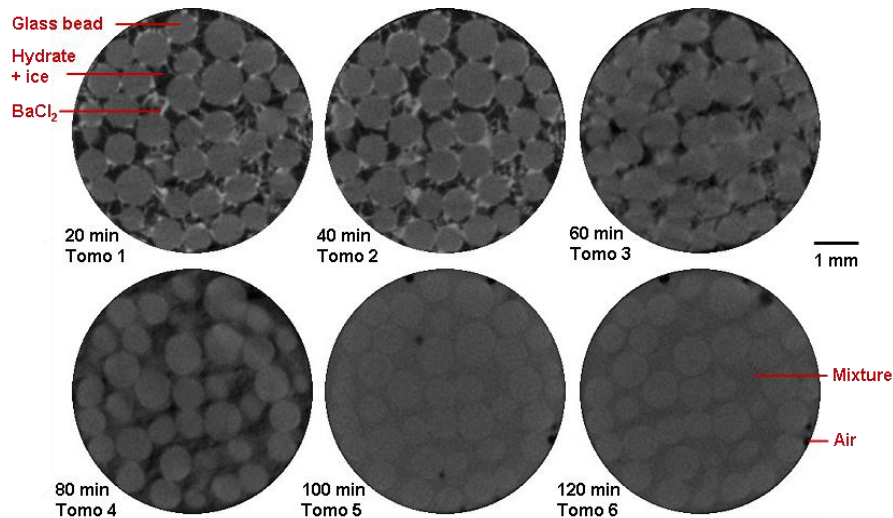


**Figure 5: Series of CT images of glass bead sample with initial hydrate saturation of 80%**

The gray values in the CT images depend on the density. Light gray and white areas represent substances with high density (barium chloride, water with barium chloride), dark gray areas show substances with low density (ice, THF hydrate).

Figure 5 shows a series of CT images for a sample with 80% hydrate saturation. The images capture the dissociation of THF hydrate. The first two tomographies indicate that THF hydrate and ice is arranged in the pore space and precipitated barium chloride covers the grain surfaces. During the imaging process, the ice melts and the resulting water in the pore space mixes with barium chloride.

Later in the data acquisition, THF hydrate dissociates. Dissociation and melting processes in the pore space cause the observed blurring in Tomographies 3 and 4. After the dissociation (Tomographies 5 and 6), the pore space is filled with a liquid mixture of all sample components (barium chloride, water, THF). We will refer to that as “mixture” in the following text. The mixture has an intermediate density and exhibits a medium gray value (Figure 6). Note that the dark gray circular spots in Tomographies 5 and 6 are air bubbles.

**Table 1: Density of sample components for  $S_h=60\%$  and 5wt%  $BaCl_2$**

| Sample component    | Water | $BaCl_2$          | $BaCl_2 +$<br>water | THF<br>hydrate    | $BaCl_2$ -water-<br>THF mixture |
|---------------------|-------|-------------------|---------------------|-------------------|---------------------------------|
| Density in $g/cm^3$ | 1.00  | 3.84 <sup>a</sup> | 1.49                | 0.97 <sup>b</sup> | 1.11                            |

<sup>a</sup> Lide and Frederikse, 1995

<sup>b</sup> Kerkar et al., 2009

For image analysis, *ImageJ* and *Matlab* were used. Image processing was used to determine which gray value in the CT images represents which substance in the sample.

Differences between the density of the components before and after dissociation are used to interpret the images. Two different images were subtracted from each other to get a gray value difference and hence a density difference. Table 1 shows the expected density values for the sample components. Density differences are negative between THF hydrate and mixture and between ice and mixture. Density differences are positive between barium chloride and mixture and between barium chloride water and mixture. Thus, images acquired before and after hydrate dissociation were subtracted to better identify the location of ice, barium chloride and THF hydrate in the images (Figures 6 and 7).

An *ImageJ* plugin called Mines Bilateral Filter is used to remove noise. The filter smoothes out gray scale differences below a chosen limit and preserves bigger, abrupt differences, such as the border between pore space and glass beads (Figure 6). A threshold of the gray scale value representing the glass beads is produced with *ImageJ*. This threshold is used to remove the glass beads from the image by setting their gray value to zero (Figure 6). The image subtraction was done by a *Matlab* program, which reads two images as 8-bit matrices. They are then converted into double matrices to prevent data loss during subtraction and to allow negative density differences. These two

double matrices are subtracted. A *Matlab* figure showing negative (blue) and positive (red) gray value differences is created (Figure 6). Then, the differential matrix is converted back to a matrix of positive integers which is exported as an 8-bit image for further analysis in *ImageJ*.

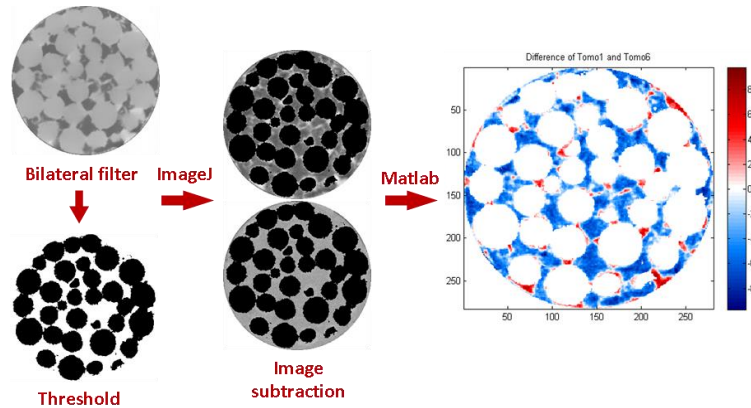


**Figure 6: Image processing workflow for MXCT images**

Figure 7 shows histograms and differential images referenced by subtracting Tomography 6 for a whole tomography series. The histogram median is shifting from low gray values to medium gray values over a series of tomographies. The number of pixels representing THF hydrate and ice (blue) and pure barium chloride or barium chloride brine (red) decreases. Pixels with intermediate gray values ( $127 \pm 20$ ) are considered either mixture or “indifferent” due to misinterpretation of pixels at the interface of high and low density areas. Figure 7 further shows that the number of pixels with intermediate gray values increases and the number of pixels with high ( $>147$ ) and low ( $<107$ ) gray values decreases during the scanning time. Areas of high gray value (red) and low gray value (blue) disappear due to dissociation of hydrate and melting of ice.

### *Ultrasonic Velocity Results*

Figure 8 shows the P and S-wave velocities recorded during the cooling of a sample which will develop 40% hydrate saturation. The velocities remain constant until hydrate formation starts. Hydrate formation results in a significant increase of velocities. The second increase in velocities is caused by the formation of ice in the sample upon further cooling. Hydrate stability and ice formation temperatures are both decreased due to the addition of barium chloride.

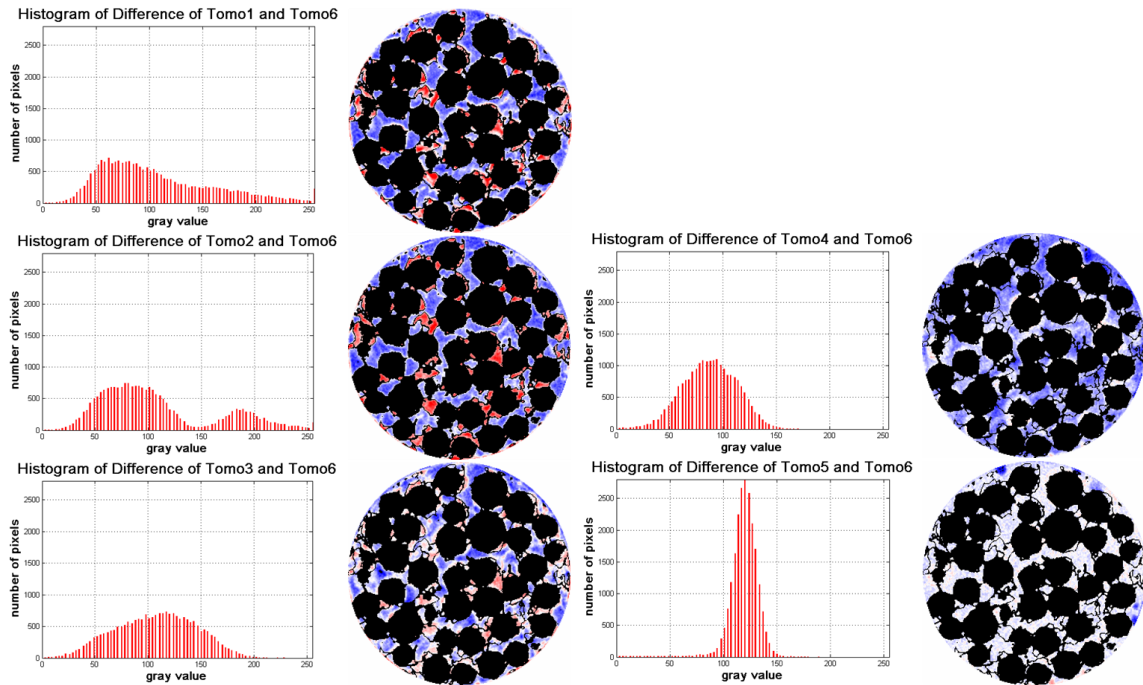


Figure 7: Histograms of gray values and differential CT images for a sample with 80% initial hydrate saturation

Figure 7 shows that the pore space appears mainly white for Tomography 5 meaning all hydrate is dissociated. The remaining blue areas in Tomography 5 are air bubbles.

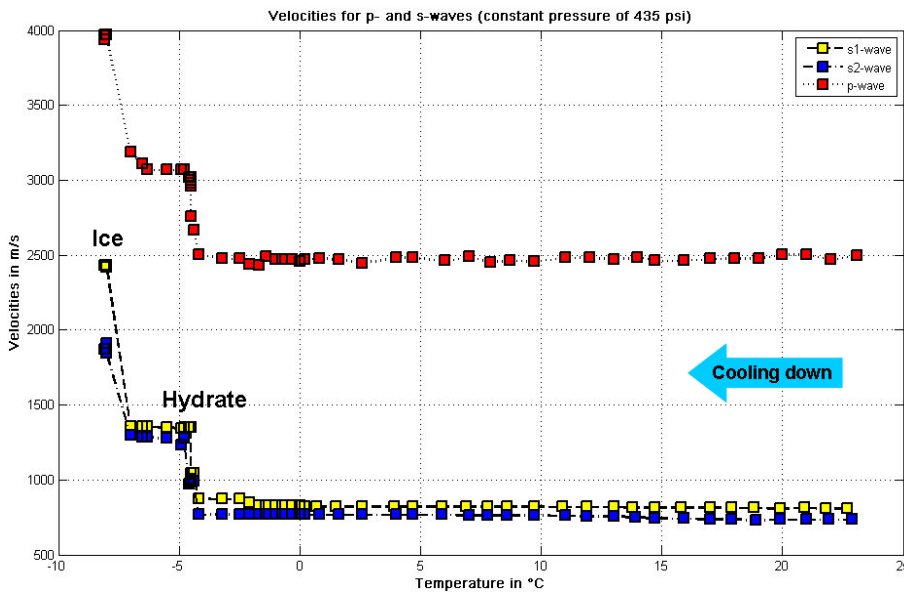


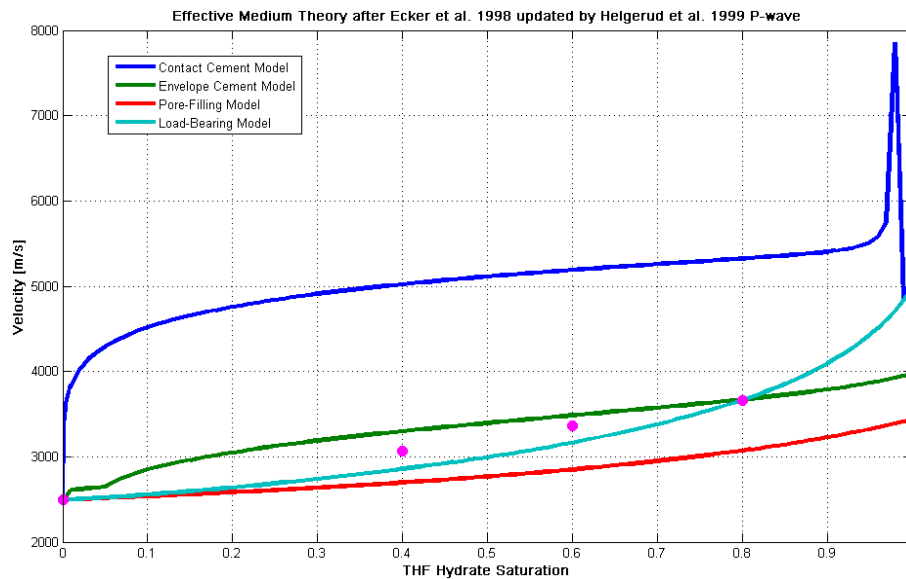
Figure 8: Velocities of P-, S1- and S2-wave for a sample with  $S_h=40\%$



Figure 9 displays velocities recorded during the cooling process for four different hydrate saturations. The velocity increase depends on hydrate saturation: the more hydrate there is in the pore space, the higher is also the increase in velocity caused by hydrate formation (Table 2). Hydrate formation starts at lower temperatures for lower hydrate saturation (Figure 9). This observation confirms that hydrate stability decreases with decreasing hydrate saturation (Makino et al., 2005).

**Table 2: Ultrasonic velocities after hydrate formation**

| Hydrate saturation | P-wave velocity | S1-wave velocity | S2-wave velocity |
|--------------------|-----------------|------------------|------------------|
| 40%                | 3070 m/s        | 1356 m/s         | 1296 m/s         |
| 60%                | 3368 m/s        | 1438 m/s         | 1417 m/s         |
| 80%                | 3656 m/s        | 1616 m/s         | 1498 m/s         |
| 100%               | 4409 m/s        | 1851 m/s         | 1874 m/s         |



**Figure 9: Effective medium model with P-wave velocities obtained by the ultrasonic measurements (pink dots), the spike in the contact cementing model is a modelling artefact**

## **Nuclear Magnetic Resonance (NMR) Investigation**

As noted previously, the development and calibration of hydrate models relies critically on the knowledge of the content of the pore space. Even small amounts of liquid or gas will have a major impact on the elastic properties. Hence, Nuclear Magnetic Resonance measurements are now being employed to characterize samples.

To initiate our investigation, we measured different types of pure fluids. First of all, we measured pure THF and the inversion results for the spectrum show that THF itself has a very strong signature in NMR measurements. Next we measured the used THF-Water mixture and when we compare it with the pure THF we can see a drop in amplitude and a faster relaxation time (a shift to the left can be seen). In Figure 10 we can see the average echo amplitudes over time recorded for THF, THF-water, and the three THF-hydrate bearing measurements.

First of all, we can see that THF signal needs a much longer time to come to zero compared to all the other samples which means the relaxation for THF compared for all the other measurements is longer. Also, when we look at the three THF-hydrate samples we can see that with increasing dissociation the amplitudes increase which are in a direct relation to the volume of fluid in the sample.

The used THF-Water ratio would, in theory, result in a 100 % THF-hydrate conversion. The reason behind these measurements was to see if we can see residual water or even residual THF within the 100 % THF-hydrate samples. If we are able to pick up a water signal during our experiments we know that not all of water and THF was converted into hydrates and we have small areas between the THF-hydrates where we have trapped water or even THF.

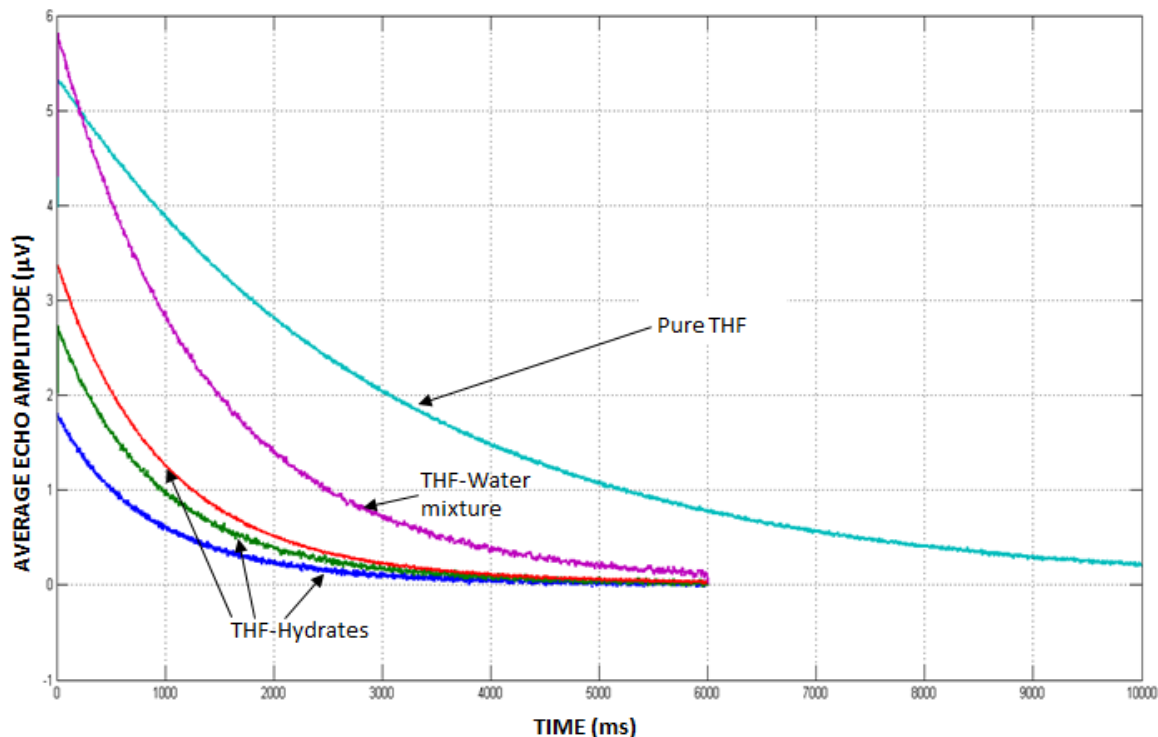


**Figure 10: Raw NMR data for THF, THF-water mixtures, and various THF hydrate compounds.**

Our first results for the measured hydrate bearing sample show that we have two distinguished peaks in the spectrum. The first measurement of pure THF-hydrate (see Figure 10, RED line) shows that we have a relatively small amplitude at around 1 sec and another small peak with almost the same amplitude just below 1 ms. In our interpretation the first peak could be the signature of water that is being trapped between the THF-Hydrate crystals. The fast relaxation time can be explained by the fact that the water is in very tiny “pores” and therefore trapped which results in a fast relaxation. The second peak could already be a THF-water mixture. It was observed that the THF hydrates started to dissociate right when they were taken out of the cooling bath. Even though we put them in a cooled container to transport them to the NMR machine, a small liquid phase started to build up.

The result for the light blue line was obtained from the same sample but at a later time (3 min after the first run was done). As we can see the first peak loses amplitude whereas the second one increases in amplitude. This could be simply a result of the dissociation process itself. The THF-hydrate continues to dissociate therefore less water is trapped in between the crystals and we have more THF-water mixture.

The purple line shows the results for a measurement performed after the light blue measurement (5 min after). Again the dissociation process continues which results in a decrease in trapped water (first peak) and an increase in THF-water (second peak). Also we start to see a shift in the second peak toward the complete dissociated sample

mentioned earlier. If we would have continued our experiments we would have expected to see a further decrease for the first peak and a continuous increase and shift of the second peak. In the case that all of the THF-hydrates would have dissociated that sample should have looked like the result of the THF-water mixture.

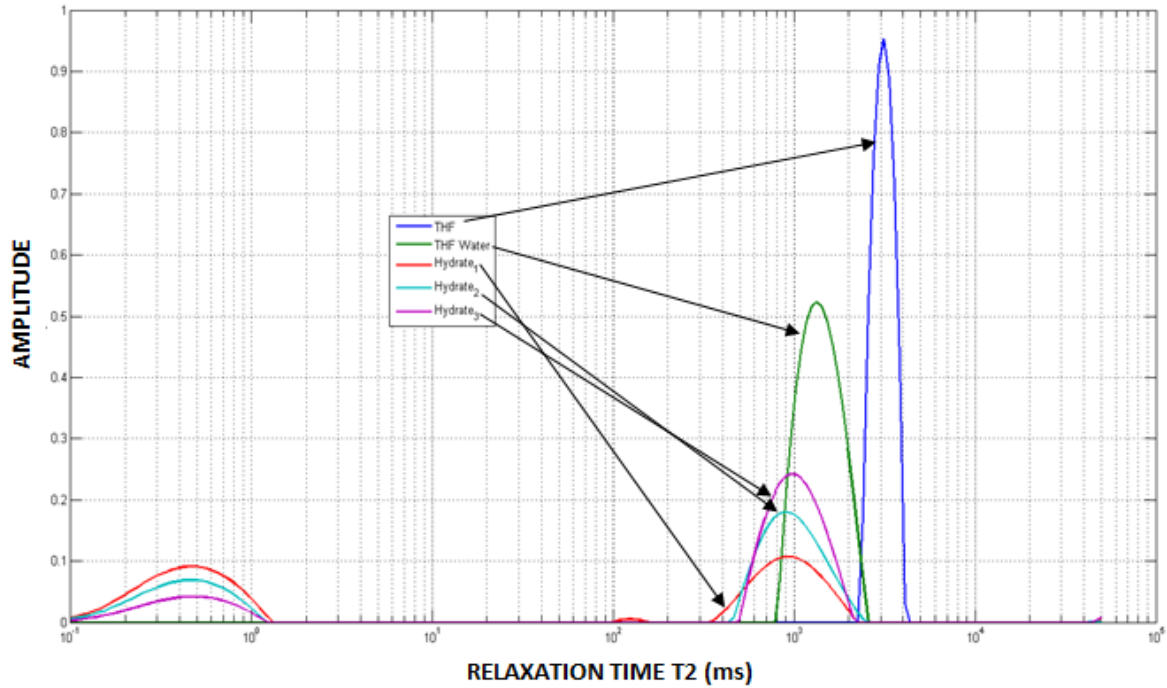


**Figure 11: Derived T2 relaxation times for the THF mixtures and hydrate compounds.**

More NMR measurements are planned for pure ice, frozen samples with 100 % THF hydrates and 100 % THF hydrates (with a better cooling transport to the NMR device).

### *Plans*

The next step forward will be the simultaneous acquisition of ultrasonic velocities and MXCT images. For this purpose, a pressure vessel needs to be installed in the CT scanner. The pressure vessel is made of glass-filled polycarbonate, a material with low X-rays absorbance. This setup provides control of temperature and pressure, thus experiments with methane hydrate can be conducted. Different formation methods will be compared with regard to their influence on pore space distribution and ultrasonic velocities of gas-hydrate bearing sediments. The setup further offers the possibility to scan samples with hydrate and barium-chloride water in the pore space but without ice. This sample composition enables us to quantify hydrate saturation.

MXCT imaging and ultrasonic velocity measurements in conjunction have the potential to enhance understanding of the influence of pore-scale hydrate distribution on ultrasonic velocities.

### **Participants and Collaborating Organizations**

Name: George Radziszewski

Project Role: Research Faculty

Nearest person month worked this period: 1.5

Contribution to Project: Dr. Radziszewski spent his time establishing standards and procedures for running the MicroCT scanner .

Funding Support: "Organics, Clays, Sands and Shales (OCLASSH) consortium

Collaborated with individual in foreign country: No

Country(ies) of foreign collaborator: N/A

Travelled to foreign country: Yes

If traveled to foreign country(ies): Poland

Duration of stay: 2 weeks

Name: Mathias Pohl

Project Role: Graduate Student

Nearest person month worked this period: 3

Contribution to Project: Mr. Pohl prepared samples and collected ultrasonic data.

Additional Funding Support: N/A

Collaborated with individual in foreign country: No

Country(ies) of foreign collaborator: N/A

Travelled to foreign country: No

If traveled to foreign country(ies),

duration of stay: N/A

Name: Mandy Schindler

Project Role: Graduate Student

Nearest person month worked this period: 3

Contribution to Project: Ms Schindler prepared samples and collected CT data.

Additional Funding Support: N/A

Collaborated with individual in foreign country: No

Country(ies) of foreign collaborator: N/A

Travelled to foreign country: No

If traveled to foreign country(ies),

duration of stay: N/A

Name: Weiping Wang

Project Role: Laboratory Technician

Nearest person month worked this period: 0 (just started involvement)

Contribution to Project: Mr. Wang assisted in equipment fabrication

Additional Funding Support: N/A  
Collaborated with individual in foreign country: No  
Country(ies) of foreign collaborator: N/A  
Travelled to foreign country: Yes  
If traveled to foreign country(ies), N/A  
duration of stay: N/A

Name: Michael Batzle  
Project Role: Principle Investigator  
Nearest person month worked: 1  
Contribution to Project: Overall (dis)organization.  
Funding Support: Academic faculty  
Collaborated with individual in foreign country: No  
Country(ies) of foreign collaborator: N/A  
Travelled to foreign country: N/A  
If traveled to foreign country(ies):

External Collaborations:  
Dr. Tim Collett  
US Geologic Survey  
Denver, Colorado: (if foreign location list country)  
Support: Data and guidance on interpretation and application  
Tim continues to publish numerous papers on hydrate properties

### **Changes / Problems**

Ms. Marisa Rydzy will defend her PhD thesis December 4, 2013. After graduation she will move to Shell Inc. in Houston. To maintain progress on the project, two graduate students and a laboratory technician are working on this project. The CT scanner will undergo maintenance to adjust and calibrate components and upgrade acquisition and analysis software. These maintenance charges will be sponsored primarily by other institutional funds as part of our cost share.

### **Special Reporting Requirements**

None

### **Budgetary Information**

Attached separately

## References

- Anderson, B. J., et al., (2008). “Analysis of Modular Dynamic Formation Test Results from the Mount Elbert 01 Stratigraphic Test Well, Milne Point Unit, North Slope, Alaska.” *Proceedings of the 6th International Conference on Gas Hydrates*, 10
- Boswell, R., Collett, T. S., (2006). “The Gas Hydrates Resource Pyramid.” *Fire in the Ice: Methane Hydrate Newsletter*, Fall issue, p. 5–7
- Boswell, R., Kleinberg, R., Collett, T. S., Frye, M., (2007). „Exploration Priorities for Marine Gas Hydrate Resources.” *Fire in the Ice: Methane Hydrate Newsletter*, Spring/Summer issue, p. 11–13
- Carroll, J. (2009) *Natural Gas Hydrates A Guide for Engineers*, 2nd ed., Elsevier, Burlington
- Collett, T. S., Johnson, A. H., Knapp, C. C., Boswell, R. (2009). “Natural Gas Hydrates: A Review.” *Natural gas hydrates—Energy Resource Potential and Associated Geologic Hazards: AAPG Memoir*, 89, p. 146– 219.
- Collett, T. S., and Ladd, J. (2000). “Detection of Gas Hydrate with Downhole Logs and Assessment of Gas Hydrate Concentrations (Saturations) and Gas Volumes on the Blake Ridge with Electrical Resistivity Log Data.” *Proceeding of the Ocean Drilling Program, Scientific Results*, 164: 179–191.
- Dallimore, S. R., Wright, J. F., Nixon, F. M., Kurihara, M., Yamamoto, K., Fujii, T., Fujii, K., Numasawa, M., Yasuda, M. Imasato, Y. (2008). “Geologic and Porous Media Factors Affecting the 2007 Production Response Characteristics of the JOGMEC/NRCAN/AURORA Mallik Gas Hydrate Production Research Well.” *Proceedings of the 6th International Conference on Gas Hydrates*, 10
- Ecker, C., Dvorkin, J., Nur, A. (1998). “Sediments with Gas Hydrates: Internal Structure from AVO.” *Geophysics*, 93 (5): 1659-1669
- Helgerud, M. B., Dvorkin, J., Nur, A., Sakai, A., Collett, T. S. (1999). “Elastic-Wave Velocity in Marine Sediments with Gas Hydrates: Effective Medium Modeling.” *Geophysical Research Letters*, 26 (13), p. 2021-2024
- Lee, J. Y., Yun, T. S., Santamarina, J. C., Ruppel, C. (2007). “Observations Related to Tetrahydrofuran and Methane Hydrates for Laboratory Studies of Hydrate-Bearing Sediments” *Geochemistry Geophysics Geosystems An Electronic Journal of the Earth Sciences*, 8 (6)
- Lide, D.R. and Frederikse, H. P. R. (Eds.) (1995). *CRC Handbook of Chemistry and Physics*, 76th ed., CRC Press, Boca Raton, FL
- Pearson, C., Murphy, J., Hermes, R. (1986). “Acoustic and Resistivity Measurements on Rock Samples Containing Tetrahydrofuran Hydrates - Laboratory Analogues to Natural

- Gas Hydrate Deposits.”, *Journal of Geophysical Research*, 91 (B14), 14132-14138
- Rydz, M. B., Batzle, M. L. (2011). “Rock Physics Characterization of THF Hydrate-Bearing Sediment” *Proceedings of the 7th International Conference on Gas Hydrates*
- Sloan, E. D. & Koh, C. A. (2008), *Clathrate Hydrates of Natural Gases*. 3rd ed., CRC Press, Taylor & Francis Group, Boca Raton, FL
- Spangenberg, E., Kulenkampff, J., Naumann, R., Erzinger, J.(2005). „Pore Space Hydrate Formation in a Glass Bead Sample from Methane Dissolved in Water.” *Geophysical Research Letters*, 32, L24301, doi:10.1029/2005GL024107
- Yun, T. S. (2005). Mechanical and Thermal Study of Hydrate Bearing Sediments. Ph. D. Thesis, Georgia Institute of Technology, Atlanta, GA
- Yun, T. S., Francisca, F. M., Santamarina, J. C., Ruppel, C (2005). “Compressional and Shear Wave Velocities in Uncemented Sediment Containing Gas Hydrate.” *Geophysical Research Letters*, 32, L10609, doi:10.1029/2005GL022607



## Milestone Status

Measurement and Interpretation of Seismic Velocities and Attenuations in Hydrate-Bearing Sediments  
 DOE Award No.: DE-FE 0009963

|    |   | <b>Planned<br/>Completion</b> | <b>Actual<br/>Completion</b> | <b>Verification</b> | <b>Comments</b>       |
|----|---|-------------------------------|------------------------------|---------------------|-----------------------|
|    | <b>Milestone Title / Description</b>          | <b>Date</b>                   | <b>Date</b>                  | <b>Method</b>       |                       |
| 1  | Project Management Plan (PMP)                 | 1-Dec-12                      | 28-Nov-12                    | DOE acceptance      | Complete and approved |
| 2  | Modifications to low frequency system         | 1-Jun-13                      |                              |                     | On schedule           |
| 3  | Modeling established using EOS                | 31-May-13                     |                              |                     | On schedule           |
| 4  | Property models of hydrates complete          | 31-May-13                     |                              |                     | On schedule           |
| 5  | Logs acquired and database estab.             | 31-Dec-13                     |                              |                     | On schedule           |
| 6  | THF hydrate grown in pressure vessel          | 1-Jun-14                      |                              |                     | Ahead of schedule     |
| 7  | Methane hydrates from free gas phase          | 31-Dec-14                     |                              |                     | Planned               |
| 8  | Methane hydrates from gas in solution         | 30-Jun-15                     |                              |                     | Planned               |
| 9  | CO <sub>2</sub> replacing methane in hydrates | 30-Sep-15                     |                              |                     | Planned               |
| 10 | MXCT scans completed                          | 30-Sep-15                     |                              |                     | Continuing            |
| 11 | Effective media models complete               | 30-Sep-15                     |                              |                     | Planned               |
| 12 | Comparison to in situ data complete           | 15-Oct-15                     |                              |                     | Planned               |
| 13 | Information Dissemination                     | 31-Dec-15                     |                              |                     | Continuing            |